Structural Properties of Zinc Sulfide Polymer Nanocomposite with Alginate

A.M. Mieshkov, T.O. Berestok, L.F. Sukhodub, A.S. Opanasyuk

Sumy State University, 2, Rimsky-Korsakov Str., 40007 Sumy, Ukraine

The comparison of structural and substructural characteristics of pure zinc sulfide and biopolymer based on ZnS composite with alginate was held by scanning electron microscopy, diffraction and X-ray fluorescence spectrometry. Films and nanostructures of zinc sulfide were obtained by chemical bath deposition from an aqueous solution of zinc nitrate, sodium alginate and thiourea at 90 °C and synthesis time of 30-120 min.

It is established that condensate growth occurs through the formation of zinc sulfide nanodots followed by merging the gaps between nanograins by alginate particles. As a result of the calculation of pole density and factor orientation it is confirmed the existence of axial texture [111] in both pure ZnS films and nanocomposites. It is shown that the lattice constants of the condensates of pure ZnS vary in the range of $a = 0.53266$-0.54419 nm, while the lattice parameters of alginate consisting ZnS polymer nanocomposites are in the range of $a = 0.53490$-0.56261 nm and inextricably dependent on time of synthesis layers.

It is established that the average size of coherent scattering domains (CSD) of films of pure ZnS in the crystallographic direction [111] is weekly changed during the deposition time ($L_{(111)} = 14$-29 nm). For ZnS composed of polymer nanocomposite, CSD sizes vary in the range of $L_{(111)} = 21$-38 nm that is larger than for pure ZnS.

Keywords: Film, Nanocomposite, ZnS, Alginate, *X*-ray, Structure, Substructure, Period lattices, Coherent scattering domain size.

PACS numbers: 84.60.Jt, 73.61.Ga

1. INTRODUCTION

Biomaterials based on polymer nanocomposites are of increased scientific interest associated with the possibility of their use in medicine, cosmetology, and electronic engineering. Biopolymers, such as chitosan, collagen, alginate, have the following advantages over synthetic polymer nanocomposites: accessibility, low cost, harmlessness for the environment, etc. [1-4]. Dispersion nanoparticles of metals and semiconductors incorporated into a polymer matrix improve the basic properties of a polymer, such as mechanical strength, stability, leads to the increase in its surface area.

Sodium alginate (Alg) is a natural biopolymer, non-toxic, biologically compatible and capable of biological resorption. This polysaccharide is a salt of alginic acid. From the chemical point of view, it consists of residues of β-D-mannuronic and α-L-guluronic acids. Salts of alginate acid are good enterosorbents, which bind and remove radionuclides and heavy metals from the body and also accelerate wound healing process. Moreover, alginic acid and its salts reduce the blood cholesterol level. Compounds with alginates on direct contact do not cause irritation of the skin and mucous membranes, and do not have allergenic properties; therefore, they are widely used in medicine and cosmetology [5, 6].

Zinc sulfide nanoparticles have attracted a great attention of researchers due to the prospect of application in optoelectronics [7], catalysis and molecular recognition systems [8], possibility of use of their luminescent and fluorescent properties [9, 10]. We should note that materials based on ZnS have good biocompatibility; composites are characterized by high ultimate strength, mechanical hardness and chemical inertness that makes them indispensable for solving various problems in a rather severe environment [11]. However, despite of numerous prospects of application of semiconductor nanomaterials, impact of these materials on the environment and human health remains unclear.

In order to obtain the nanoparticles, including those based on multicomponent semiconductors, the method of chemical bath deposition from an aqueous solution, which is characterized by its simplicity and efficiency [12-17], is a promising one. Currently, this method becomes the most common way to produce stable and biocompatible composites [18], since it realizes the chemical joining of an organic-active substance to the surface of the nanocrystal during synthesis.

Composites based on zinc sulfide and sodium alginate nanoparticles are studied insufficiently; therefore, this conditioned the aim and objectives of the investigation, namely, the study of the effect of the chemical reaction duration on the structural and substructural characteristics of the obtained condensates compared with pure ZnS films. The importance of research is conditioned by the fact that high adsorption ability with respect to different microorganisms is typical for such composites [19].

2. EXPERIMENTAL DETAILS

Zinc sulfide films and nanostructures were obtained on pre-cleaned glass substrates by chemical bath deposition from an aqueous solution [20]. At that, mixture of zinc nitrate and thiourea was used as the precursor. Ammonia was added to the initial solution to increase the pH level. The chemical reactor temperature during synthesis maintained at the level of 90 °C. Solution of sodium alginate was added to the obtained mixture to form the composite of zinc sulfide and alginate. To study the effect of the synthesis time on the structural characteristics of the obtained condensates, duration of their deposition varied in the range from 30 to 120 minutes.

Microelement composition of the samples was determined using the X-ray fluorescent spectrometer "ElvaX Light SDD" (Kiev, Ukraine). The spectrometer allows to define the content of elements in the range from Na

($Z = 11$) to U ($Z = 92$), since has the beryllium window of the thickness of 140 μm. X-ray tube with a rhodium anode is the primary radiation source; anode cooling is performed by the Peltier elements. Resolution of the X-ray detector is equal to 165 eV at 5.9 keV (Mn-K$_\alpha$ line). Processing of the obtained energy spectra was carried out in the experimental support system ElvaX. Elemental analysis of the ZnS- and alginate-based composites was performed by the standard technique [21].

Structural studies of the obtained films were carried out on the automated X-ray diffractometer DRON 4-07 in Ni-filtered K$_\alpha$-radiation of the copper anode. Measurements were performed in the range of angles 2θ from 10° to 60°, where 2θ is the Bragg angle. Bragg-Brentano focusing of the X-ray radiation was used in the study [22]. Phase analysis was carried out by comparison of the interplanar spacings and relative intensity from the studied samples and standard by the JCPDS data [23].

Films texture was estimated by the Harris method, which is especially convenient in the study of planar samples with the texture axis oriented along the normal to their surface [22, 24]. The pole density was calculated by the formula $P_i = (I_i/I_{0i})/(1/N) \sum_{i=1}^{N} I_i/I_{0i}$, where I_i, I_{0i} are the integral intensities of the i-th diffraction peak for the film sample and standard, respectively; N is the number of lines presented on the X-ray pattern.

Thereafter, we plotted the dependences $P_i - (hkl)_i$ and $P_i - \varphi$, where φ is the angle between the texture axis and the normal to different crystallographic planes, to which reflections on the diffraction patterns correspond; (hkl) are the Miller indices. This angle was calculated for the cubic lattice using expressions given in [24]. The texture axis has those indices, to which the maximum value of P_i corresponds. In this case, the orientation factor for the corresponding direction can be calculated from the expression $f = \sqrt{\sum_{i=1}^{N} (P_i - 1)^2 / N}$.

Calculation of the lattice constant a was performed by the position of the $K_{\alpha 1}$-component of all the most intense lines, which were present on the diffraction patterns from the material using the following relations true for the cubic phase [24]:

$$a = \frac{\lambda}{2\sin\theta} \sqrt{(h^2 + k^2 + l^2)},$$
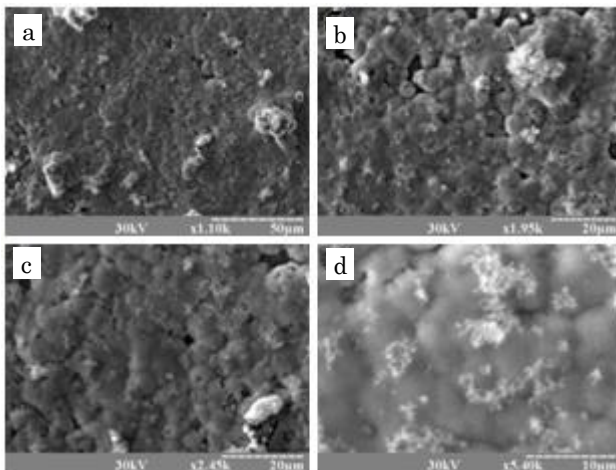
where λ is the X-ray radiation length; h, k, l are the Miller indices.

Further, in order to obtain the precision values of the lattice constant of the compound, the Nielson-Reilly extrapolation method was used. At that, the dependences $a(c) - 1/2\cos^2\theta(1/\sin\theta + 1/\theta)$ were plotted. Linear approximation of the obtained points was carried out using the least square method.

The Scherrer relation was used in order to determine the average size of the coherent-scattering regions (CSR) L in the films [22, 24]: $L = K\lambda/\beta\cos\theta$, where K is the coefficient dependent on the grain shape ($K = 0.94$); β is the physical expansion of the diffraction lines.
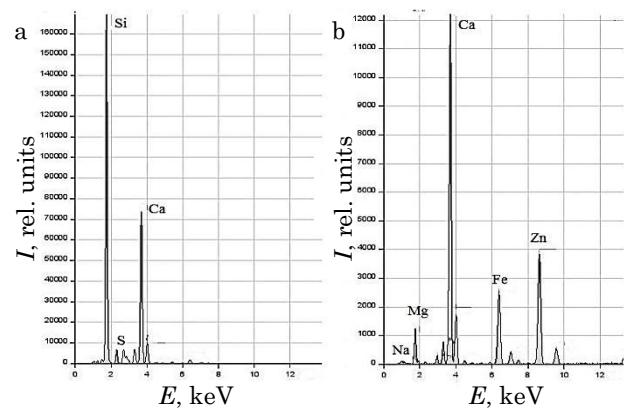
3. EXPERIMENTAL

3.1 Morphological properties of ZnS polymer nanocomposites with alginate

The electron-microscopic images of the surface of ZnS composite with alginate obtained at different deposition durations are illustrated in Fig. 1.

As seen from Fig. 1, growth of the condensate occurs by the formation of zinc sulfide nanodots followed by merging the gaps between nanograins by alginate particles. Increase in the deposition time to 120 min leads to the formation of a continuous film and further building-up of the next composite layer. Growth features of the films of pure ZnS obtained by vacuum and chemical methods are studied in our works [25-27].

The typical characteristic spectra from the film samples are represented in Fig. 2. It is established that in the samples, the deposition time of which was equal to 75 minutes, only a part of the material volume gives the contribution to the observed fluorescence strength. For thinner samples ($\tau = 30$ min), fluorescence strength dropped with decreasing sample thickness. Results of the X-ray fluorescence analysis indicate the presence of zinc sulfide particles in the studied composite. Fluorescence peaks from the elements which belong to sodium alginate or glass (Na, K, Mg, Al, Si, etc.) [28] were also present in the obtained spectra besides the lines corresponding to zinc and sulfur.

Unfortunately, it is impossible to separate the contribution to the total spectra from biopolymer and glass. Lines from ruthenium (Ru) and rhodium (Rh), which are the background spectrum of the device, are also observed in the spectrograms.

Fig. 1 – Images of the surface of ZnS films with alginate at the deposition duration of $\tau = 60$ min (a, b) and 120 min (c, d)

Fig 2 – Characteristic X-ray spectra in the region of light (a) and heavy (b) elements from polymer ZnS + Alg nanocomposites at the deposition duration 30 min

3.2 Structural characteristics of the films

The diffraction patterns from zinc sulfide films and ZnS polymer nanocomposites with alginate obtained at different deposition durations are shown in Fig. 3a, b. As a rule, reflections from the crystallographic planes (111), (220), (311) of the cubic phase (sphalerite) at the diffraction angles of $29.36° - 29.56°$, $48.32° - 48.62°$ and $57.12° - 57.22°$ were detected in the diffraction patterns [23]. In zinc sulfide films with alginate these peaks were shifted with respect to the position typical for ZnS layers without alginate that, to our opinion, is the result of the presence of alginate in the condensates and indicates the presence of stresses in the films and change in the lattice constant of the material. Reflection from the plane (111) was dominant by intensity in diffraction patterns that implies the presence of the growth texture [111] in the films.
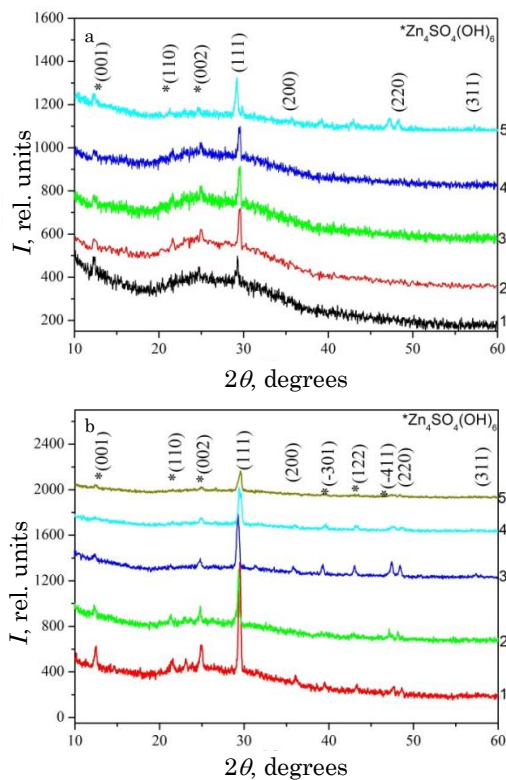

Fig. 3 – Diffraction patterns from pure ZnS films (a) and ZnS polymer nanocomposites with alginate (b) deposited at different deposition durations τ, min: $2 - 30$, $3 - 45$, $4 - 60$, $5 - 90$, $6 - 120$

Moreover, peaks at angles of $12.23°$, $21.18°$, $24.99°$, $39.31°$, $43.04°$ and $47.04°$, which we have identified as reflections from the planes (001), (110), (002), (− 301), (122), (− 411) of the hexagonal phase of $Zn_4SO_4(OH)_6$ [39-690] compound [23] were present in a number of diffraction patterns from both ZnS films and ZnS polymer nanocomposites with alginate. This can be caused by the interaction of the incoming precursors with each other and embedding of the residual products into films during their synthesis. As the literature analysis has shown, further annealing of the condensates leads to the decomposition of the given compound [29].

As a result of the calculation of the pole density and orientation factor of pure ZnS films and ZnS layers with alginate, the existence of the axial texture [111] has been confirmed (Fig. 4). Such growth texture is typical, when

producing ZnS films by vacuum and chemical deposition. For example, a similar growth texture was observed in the works [27, 30].

Dependence of the orientation factor on the deposition duration is shown at the inset of Fig. 4. As seen from the figure, texture perfection of pure ZnS films is improved (f = 1.45-1.79) with increasing deposition time and, correspondingly, condensate thickness. Moreover, growth texture perfection of ZnS polymer nanocomposites with alginate becomes slightly worse (f = 2.05-1.71) with increasing deposition time and, correspondingly, film thickness. This fact is explained by the growth features of the condensates in the presence of alginate.
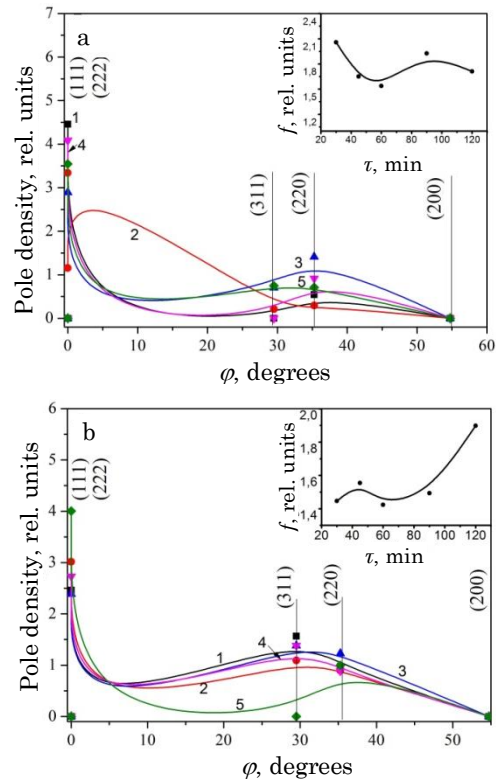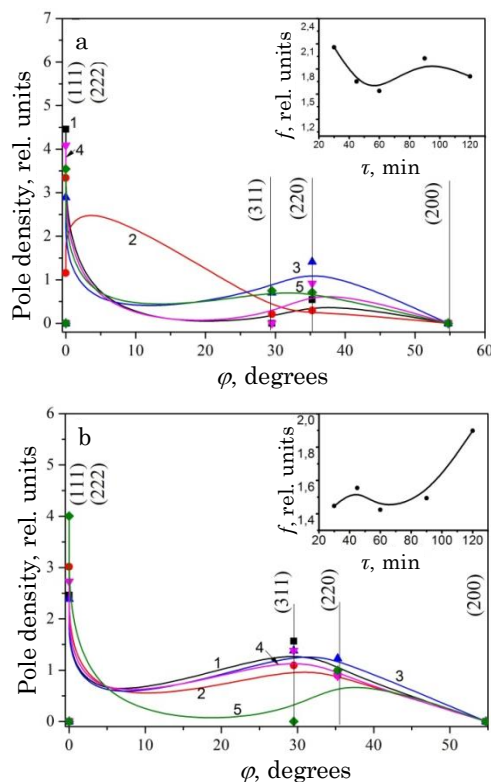

Fig. 4 – Dependence of the pole density P_i on the angle φ between the texture axis and the normal to the reflecting plane for ZnS films (a) and ZnS polymer nanocomposites with alginate (b) obtained at τ, min: 30 (1), 45 (2), 60 (3), 90 (4), 120 (5). On the inset: dependence of the orientation factor f on the time τ of the layer synthesis

Moreover, it is established that pure zinc sulfide films have a less perfect growth texture compared with ZnS films with alginate at the initial growth stages that is confirmed by the calculated values of the orientation factor for both cases (see the insets in Fig. 4a, b). From our point of view, this is explained by the fact that pure zinc sulfide films under the same production conditions were thinner and less uniform in area compared with ZnS condensates with alginate. We should also note that addition of alginate improved adhesion of the films to the glass substrate surface. Such features are probably associated with the fact that alginate molecules encapsulate zinc sulfide particles changing the state of their surface.

The results of determination of the lattice parameters of synthesized ZnS condensates and ZnS polymer nanocomposites with alginate depending on the duration of film deposition are represented in Fig. 5 and Table 1.

Table 1 – Structural and substructural characteristics of the obtained condensates

ZnS					ZnS + Alginate			
τ, min	a, nm	$V \cdot 10^{27}$, nm^3	$L_{(111)}$, nm	$L_{(220)}$, nm	a, nm	$V \cdot 10^{27}$, nm^3	$L_{(111)}$, nm	$L_{(220)}$, nm
30	0.54419	0.1612	21.5	56.3	0.53490	0.1530	28.7	30.0
45	0.53602	0.1540	20.6	23.8	0.55252	0.1687	37.7	40.8
60	0.53266	0.1511	17.2	49.4	0.54261	0.1598	24.5	25.8
90	0.53845	0.1561	28.9	26.2	0.56261	0.1781	20.9	12.5
120	0.53758	0.1554	13.8	75.0	0.54281	0.1599	20.3	29.3
[23]	0.54060	0.1574	–	–	–	–	–	–

Fig. 4 – Dependence of the pole density P_i on the angle φ between the texture axis and the normal to the reflecting plane for ZnS films (a) and ZnS polymer nanocomposites with alginate (b) obtained at τ, min: 30 (1), 45 (2), 60 (3), 90 (4), 120 (5). On the inset: dependence of the orientation factor f on the time τ of the layer synthesis

Dotted line in the figure denotes the values of the lattice constant of the material given in the reference book for zinc sulfide monocrystals [23].

The calculations have shown that the values of the lattice constants of condensates of pure ZnS varied in the range of $a = 0.53266$-0.54419 nm. These values slightly differed from the reference ones ($a = 0.5406$ nm) at short deposition duration ($\tau = 30$-60 min) and approached them ($a = 0.54419$ nm) with increasing chemical reaction time ($\tau = 120$ min).

It is seen from Fig. 5 that the lattice constant of ZnS layers, being a part of the polymer nanocomposite with alginate, substantially differs from the reference data for the bulk material varying in the range of $a = 0.53490$-0.56261 nm. Obviously, this effect is conditioned by the presence of alginate macromolecules in the condensate. With increasing deposition time, the values of the lattice constant of the material ($a = 0.56261$ nm) begin to significantly exceed the reference values.

Calculation of the volume of the ZnS cubic cell in the obtained films was performed based on the measurement results of the crystal lattice constants of a two-component compound (Fig. 5). The calculations indicate that the values of the crystal lattice volume decrease with chemical reaction ($V = 0.161 \cdot 10^{-27}$ m^3-$0.155 \cdot 10^{-27}$ m^3). It is established that in the ZnS polymer nanocomposites with alginate, the increase in the layer deposition time from $\tau = 30$ min to $\tau = 90$ min leads to the increase in the crystal lattice volume of the material from the value of $V = 0.150 \cdot 10^{-27}$ m^3 to $V = 0.178 \cdot 10^{-27}$ m^3; and further increase in the chemical reaction duration leads to some decrease in this volume to $V = 0.160 \cdot 10^{-27}$ m^3 and, correspondingly, approximation of the obtained values to the reference ones ($V = 0.157 \cdot 10^{-27}$ m^3).

3.3 Substructural properties of the condensates

Calculation results of the CSR sizes in the directions perpendicular to the crystallographic planes (111) and (220) are presented in Table 1. As seen from the table, the average CSR sizes of the pure ZnS films in the [111] direction is weakly changed in the whole range of the studied deposition time ($L_{(111)} = 14$-29 nm). For the ZnS, being a part of the polymer nanocomposite with alginate, it is established that the CSR sizes are in the range of $L_{(111)} = 21$-38 nm. As seen from Table 1, increase in the time of the film deposition leads, firstly, to the significant increase in the CSR sizes from $L_{(111)} = 28.7$ nm to $L_{(111)} = 37.7$ nm, however, with further deposition of the condensates (120 min), their decrease to 20.3 nm takes place. The maximum value of the CSR size is observed in the layers obtained at the deposition time of $\tau = 45$ min ($L_{(111)} = 37.7$ nm). On average, the CSR size in the [111] direction in ZnS, being a part of the polymer nanocomposite with alginate, was larger than in pure ZnS. The authors of [31] obtained similar values of the CSR sizes $L_{(111)} = 22$-53 nm for the condensates produced by the magnetron sputtering method using the Scherrer formula. The influence of the deposition time on the CSR sizes in the direction [220] in the films of pure ZnS and the compound, being a part of the polymer nanocomposite, can be traced in Table 1.

The previous studies of the bactericidal activity of the zinc sulfide samples with alginate relative to the tested strains of microorganisms (Peptostreptococcusanaerobius, Streptococcuspyogenes, Bacteroidesfragilis) indicate their antimicrobial action against all gram-positive and gram-negative test cultures.

4. CONCLUSIONS

1. The comparative analysis of the structural and substructural characteristics of the pure zinc sulfide films

and a biopolymer based on ZnS composite with alginate obtained by the chemical bath deposition from an aqueous solution of zinc nitrate, thiourea and sodium alginate at the temperature of 90 °C and different synthesis times has been performed.

2. It is established that the condensate growth occurs through the formation of zinc sulfide nanodots followed by merging the gaps between grains by alginate particles. Increase in the deposition time up to 120 min leads to the formation of a continuous film and further building up of the next composite layer.

3. Existence of the axial texture [111] in pure ZnS films and ZnS films with alginate was confirmed by the calculation results of the pole density orientation factor. It is established that texture perfection of ZnS films is improved ($f = 1.45$-1.79) with increasing deposition time, while the growth texture perfection of ZnS polymer nanocomposites with alginate becomes worth in this case ($f = 2.05$-1.71). Zinc sulfide film at the initial growth stages have less perfect growth texture compared with ZnS films with alginate.

4. It is shown that the values of the lattice constants of the pure ZnS condensates were changed in the range of $a = 0.53266$-0.54419 nm. These values slightly differed from the reference values ($a = 0.5406$ nm) at short deposition time ($\tau = 30$-60 min) and approached the refer

ence ones ($a = 0.54419$ nm) with increasing time of the chemical reaction ($\tau = 120$ min). The lattice constant of ZnS layers, being a part of the polymer nanocomposite with alginate, significantly differs from the reference data for a bulk sample and is changed in the range of $a = 0.53490$-0.56261 nm and inextricably dependent on the synthesis time.

5. It is established that the average CSR sizes for pure ZnS films in the direction [111] are weakly changed in the whole range of the investigated deposition time of the films ($L_{(111)} = 14$-29 nm). For the ZnS, being a part of the polymer nanocomposite with alginate, CSR sizes belong to the range of $L_{(111)} = 21$-38 nm. On average, CSR size in the direction [111] in the ZnS, being a part of the polymer nanocomposite with alginate, was larger than in pure zinc sulfide.

ACKNOWLEDGEMENTS

REFERENCES

1. H. Mittal, E. Fosso-Kankeu, S. Mishra, A.K. Mishra, *Int. J. Biol. Macromol.* **62**, 370 (2012).
2. S. Ghorai, A. Sinhamahpatra, A. Sarkar, A.B. Panda, S. Pal, *Bioresour. Technol.* **119**, 181 (2012).
3. S.S. Banerjee, D.H. Chen, *J. Hazard. Mater.* **147**, 792 (2007).
4. Y.C. Chang, D.H. Chen, *J. Colloid Interface Sci.* **283**, 446 (2005).
5. R.A. Aziz, N. Asyikin, I. Sopyan, *J. Inst. Eng.* **70**, 34 (2009).
6. Y. Wang, H. Cheng, L. Zhang, Y. Hao, J. Ma, B. Xu, W. Li, *J. Mol. Catal. A: Chem.* **151**, 205 (2000).
7. N.A. Smol'yaninov, *Pprakticheskoye rukovodstvo po mineralogii* (M.: Nedra: 1972).
8. S. Suryajaya, A.V. Nabok, A.K. Hassan, A. Tsargorodskaya, *Jurnal Fisika dan Aplikasinya* **7**(1) 110107-1 (2011).
9. H. Kimetal, *IEEE Nanotechnol. Magazine* **6** No 1, 19 (2012).
10. W. Vogel, P.H. Borse, N. Deshmukh, S.K. Kulkarni, *Langmuir* **16**, 2032 (2000).
11. M. Labrenz, G.K. Druschel, T. Thomsen-Ebert, B. Gilbert, S.A. Welch, K.M. Kemner, *Science* **290**, 1744 (2000).
12. H.J. Lee, S.I. Lee, *Curr. Appl. Phys.* **7**, 193 (2007).
13. F. Long, W.M. Wang, Z. Cui, L.Z. Fan, Z. Zou, T. Jia, *Chem. Phys. Lett.* **462**, 84 (2008).
14. A.U. Ubale, D.K. Kulkarni, *Bull. Mater. Sci.* **28**, 43 (2005).
15. Q. Liua, M. Guobing, A. Jianping, *Appl. Surface Sci.* **254**, 5711 (2008).
16. T. Ben Nasr, N. Kamoun, C. Guasch, *Mater. Chem. Phys.* **96**, 84 (2006).
17. A.S. Opanasyuk, T.O. Berestok, P.M. Fochuk, A.E. Bolotnikov, R.B. James, *Proc. of SPIE* **8823**, 88230Q (2013).
18. T.O. Berestok, D.I. Kurbatov, A.S. Opanasyuk, N.M. Opanasyuk, V.M. Kuznetsov, *Proc. 22st Int. Crimean Conf.: Microwave and Telecommunication Technology*, 693 (CriMiCo 2012).
19. Zhulai Li, Peng Chen, Xiuzhi Xu, Xiao Ye, Jin Wang, *Mater. Sci. Eng. C* **29**, 2250 (2009).
20. T.O. Berestok, D.I. Kurbatov, N.M. Opanasyuk, et al., *J. Nano-Electron. Phys.* **5** No 1, 01009 (2013).
21. N.F. Losev, *Osnovy rentgenospektral'nogo fluorestsentnogo analiza* (M.: Khimiya: 1982).
22. B.E. Warren, *X-ray Diffraction* (New York: Dover: 1990).
23. *Selected powder diffraction data for education straining (Search manual and data cards), Published by the International Centre for diffraction data*, 432 (1997).
24. Ja.S. Umanskij, Ju.A. Skakov, A.N. Ivanov, L.N. Rastorgujev, *Crystallogaphy, X-ray graph and electronmicroscopy* (M.: Metallurgy: 1982).
25. D.I. Kurbatov, A.S. Opanasyuk, H. Khlyap, *phys. status solidi a* **206** No 7, 1549 (2009).
26. D. Kurbatov, A. Opanasyuk, S. Duvanov, et al., *Solid State Sci.* **13**, 1068 (2011).
27. A.S. Opanasyuk, D.I. Kurbatov, V.V. Kosyak, et al., *Crystallography Reports* **57** No 7, 927 (2012).
28. G.B. Harris, *Philosophical Magazine Series* 7 **43**, 113 (1952).
29. R. Zhang, B. Wang, L. Wei, *Vacuum* **82**, 1208 (2008).
30. C.J. Panchal, A.S. Opanasyuk, V.V. Kosyak, M.S. Desai, I.Yu. Protsenko. *J. Nano- Electron. Phys.* **3** No 1, 274 (2011).
31. Dong Hyun Hwang, Jung Hoon Ahn, Kwun Nam Hui, Kwan San Hui, Young Guk Son, *Nanoscale Res. Lett.* **7** No 1, 26 (2012).